Short-Term Changes in Cerebral Microhemodynamics after Carotid Stenting

Iain D. Wilkinson, Paul D. Griffiths, Nigel Hoggard, Trevor J. Cleveland, Peter A. Gaines, Sumaira Macdonald, Fiona McKevitt and Graham S. Venables

AJNR Am J Neuroradiol 2003, 24 (8) 1501-1507
http://www.ajnr.org/content/24/8/1501

AJNR Am J Neuroradiol 24:1501–1507, September 2003

Short-Term Changes in Cerebral Microhemodynamics after Carotid Stenting

Iain D. Wilkinson, Paul D. Griffiths, Nigel Hoggard, Trevor J. Cleveland, Peter A. Gaines, Sumaira Macdonald, Fiona McKevitt, and Graham S. Venables

BACKGROUND AND PURPOSE: **The cerebral hemodynamic sequelae of interventions in patients with severe internal carotid artery (ICA) stenoses are not fully understood. In this study, we sought to determine the immediate changes in cerebral perfusion characteristics, determined by MR imaging in patients who have undergone unilateral transluminal angioplasty and stent placement.**

METHODS: **Eleven patients with symptomatic high-grade ICA stenosis underwent MR imaging within 4 hours before and within 3 hours after carotid stent placement. First-pass gadolinium-enhanced imaging of perfusion was performed by using a gradient-recalled echo-planar technique. Localized relative cerebral blood volume (rCBV) and bolus first-moment transit time (TT_{FM}) were calculated for different vascular territories (middle, anterior, and posterior cerebral arteries) in each hemisphere.**

RESULTS: **Significantly longer TT_{FM} ($P < .005$) was observed in the symptomatic territory of the middle cerebral artery before intervention. After intervention, TT_{FM} remained significantly longer in this territory ($P < .05$). However, the magnitude of the interhemispheric asymmetry had declined significantly (50–60% reduction; $P < .05$). No significant differences or changes in rCBV were identified between hemispheres, between images, or in areas of unilateral leptomeningeal enhancement after intervention.**

CONCLUSION: **MR can demonstrate short-term partial resolution of timing asymmetry in interhemispheric perfusion after angioplasty and stent insertion for severe stenosis of the ICA.**

Interventional procedures aimed at reducing the risk of stroke in patients with severe stenosis of the internal carotid arteries (ICAs) include surgical endarterectomy (1, 2), percutaneous transluminal angioplasty (PTA) (3), and a combination of angioplasty with endovascular stent insertion (4). Whether the reductions in stroke risk afforded by these interventional procedures wholly result from a reduced embolism rate, from improved cerebral blood flow, or from a combination of the two remains unproven. Parenchymal vulnerability to the presence of emboli may itself be influenced by blood flow (5). Knowledge of the arterial perfusion characteristics before and after treatment for ICA stenosis may aid our understanding of the risks of stroke and of the hemodynamic complications associated with intervention.

Advances in MR technology have enabled the in vivo acquisition of high-quality multisection echo-planar images of the cerebrum with subsecond temporal resolution. Chelates of gadolinium (6), a rare earth metal, are commonly used as exogenous contrast agents in MR imaging. These chelates have a modulatory effect on both the T1 and T2* of tissue within their sphere of influence. Coupled with a fast T2*-weighted imaging technique, the detection of the passage of a bolus of exogenous contrast agent as it passes through the capillary bed provides a method for spatially mapping the perfusion characteristics of the cerebral parenchyma (7–9).

This study used a dynamic contrast-enhanced MR perfusion technique to assess the short-term (<3 hours) cerebral microhemodynamic consequences of PTA and stent insertion in a group of patients with severe, symptomatic atherosclerotic disease of the ICA. Leptomeningeal enhancement over the hemisphere ipsilateral to the side of stent placement has previously been reported (10). This study was also conducted to specifically assess for perfusion changes in regions demonstrating such enhancement.

Received December 11, 2002; accepted after revision March 6, 2003.

From the Academic Unit of Radiology, University of Sheffield (I.D.W., P.D.G., N.H.) and Sheffield Vascular Institute, Sheffield Teaching Hospitals (T.J.C., P.A.G., S.M., F.M., G.S.V.), England.

Presented in part at the 39th Annual Meeting of the American Society of Neuroradiology, Boston, MA, 2001.

Address reprint requests to Dr I. D. Wilkinson, Academic Unit of Radiology, C Floor, Royal Hallamshire Hospital, Glossop Road, Sheffield, England S10 2JF.

TABLE 1: Patient Demographic Data and Interval Between MR Examinations

Subject/Sex/Age, y	Presenting Symptoms	ICA Stenosis, %		Time between MR Examinations, h:min
		Symptomatic Side	Asymptomatic Side	
1/F/74	Amaurosis fugax	90	0	06:31
2/M/58	Nondisabling stroke	95	50	03:59
3/F/72	Amaurosis fugax	85	<30	03:52
4/F/61	Transient ischemic attack	95	<30	03:39
5/F/79	Transient ischemic attack	90	<30	02:13
6/M/71	Transient ischemic attack	85	50	02:57
7/F/75	Amaurosis fugax	80	70	04:30
8/M/58	Nondisabling stroke	66	0	06:16
9/M/71	Transient ischemic attack	80	0	03:07
10/M/62	Minor stroke	95	30	06:13
11/M/76	Amaurosis fugax	90	0	03:17

Methods

Subjects

The study group consisted of six men and five women (mean age, 69 years; range, 58–79 years) who had symptoms consistent with cerebral or retinal ischemia or infarction (Table 1). The recruitment and investigative protocols were approved by the local research ethics committee, and all subjects provided written informed consent before their participation in this study. Patients were assessed with initial screening with Doppler sonography and then conventional angiography if sonography showed an ICA stenosis of greater than 50%. Angiography was performed to confirm the presence of severe carotid bifurcation stenosis and to look for significant atherosclerotic disease of the aortic arch, its branches, and the intracranial arterial system. Patients with severe stenosis in the ICA (according to the North American Symptomatic Carotid Endarterectomy Trial criteria [1]) and without significant disease other than that at the level of the carotid bifurcation (ie, an absence of significant tandem lesions) were recruited into this study. One of the patients (number 9) had undergone previous carotid stent insertion on the opposite side to that being treated during this study. Table 1 shows the degree of ICA stenosis ipsilateral and contralateral to the patients' symptomatic side, with the patient demographic data and the interval between MR examinations.

MR Examinations

MR examinations were performed on a 1.5-T system (Eclipse; Philips Medical Systems, Cleveland, OH) within 4 hours before and less than 3 hours after stent placement. The MR protocol included the acquisition of axial images of the brain by using a dual-echo fast spin-echo technique (TR/TE, 2000/20 and 90) and fluid-attenuated inversion-recovery (FLAIR) technique (TR/TE/TI, 6000/95.9/1800). The latter was performed both before and after the perfusion assessment.

Indirect indicators of parenchymal perfusion were assessed by using a multi–time point, single-shot T2*-weighted echo-planar sequence (TR/TE_{eff},1400/60; acquisition matrix,192 × 188 zero-filled before Fourier transformation to 256 × 256; FOV, 25 cm). Twelve 5-mm-thick contiguous axial sections were acquired over the cerebrum every 1.4 seconds for a total imaging time of 98 seconds, yielding 70 time points. Exogenous perfusion contrast was provided by a 20-mL bolus of gadolinium diethylenetriamine pentaacetic acid (Magnevist; Schering, Berlin, Germany) (6). The bolus was followed by a 20-mL sodium chloride flush administered intravenously by using a power injector (Spectris; Medrad, Beek, the Netherlands) at a rate of 5 mL/s starting on the 10th imaging time-point.

Post-acquisition processing was performed by using software integrated with the imaging system, in a manner similar to that described elsewhere (11). As the bolus of gadolinium chelate passes through a region of interest (ROI), a loss in signal intensity occurs as the transverse relaxation rate (R_2*) increases as a result of localized signal dephasing. For each imaging episode, the timing of the signal-intensity change within user-defined ROIs was obtained with respect to those defined by the signal-intensity time-course of a circular ROI placed within the proximal intracranial ICA on the asymptomatic side (Fig 1A). Four hemodynamic anatomic ROIs (Fig 2) were defined in each cerebral hemisphere as follows: posterior cerebral artery territory (PCAT), middle cerebral artery (MCA) territory at the level of the lateral ventricles (MCAT1), MCA territory superior to the lateral ventricles (MCAT2), and anterior cerebral artery territory (ACAT). In addition, if unilateral leptomeningeal enhancement was observed on FLAIR images obtained after intervention and before the second perfusion run, ROIs were placed over the underlying cortical gyri, both ipsilateral and contralateral to the area of enhancement. The signal time-course of the average pixel value within an anatomic ROI, $S(t)$, was inverted and a gamma-variate fitted to this experimental data (to minimize influences of recirculation [12]) by using a nonlinear least-square fitting procedure (Fig 1B). The fitted concentration time curve, $C(t)$, for this ROI is given by Equation 1:

$$C(t) = -(k/TE_{eff})\ln[S(t)/S(t=0)], \quad (1)$$

where k is a constant and TE_{eff} is the effective TE. The concentration time-curve is directly proportional to the change in transverse relaxation rate, ΔR_2*, at time t bought about by the proximity of the gadolinium ion as it passes through the capillary bed, as shown in Equation 2:

$$C(t) \propto \Delta R_2^*(t). \quad (2)$$

Two variables were used to characterize $C(t)$. These were related to the local blood volume and to flow: rCBV, (the area under the fitted curve) and the first moment (or the mathematical center of mass) ofthe fitted gamma-function, as defined by Equations 3 and 4, respectively:

$$\mathrm{rCBV} = \int_0^\infty C(t)\mathrm{d}t \quad (3)$$

and

$$\mathrm{TT_{FM}} = \int_0^\infty C(t).t\mathrm{d}t \div \int_0^\infty C(t)\mathrm{d}t. \quad (4)$$

To facilitate comparisons between data acquired before intervention and data acquired after intervention, values of

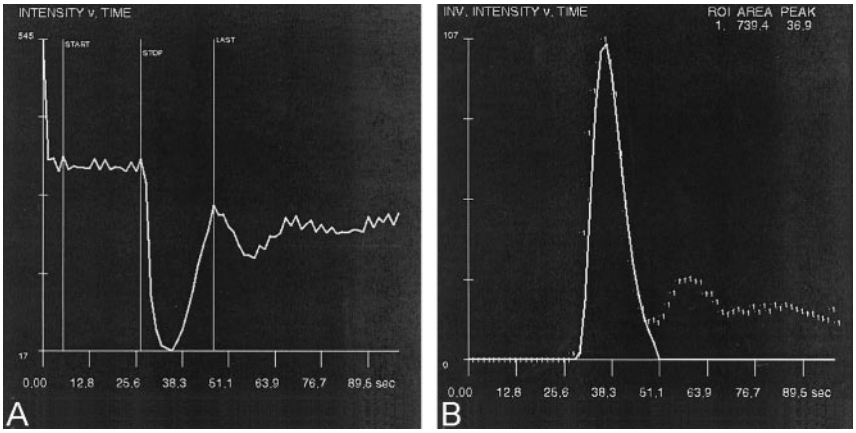

FIG 1. Signal intensity versus time.

A, Mean signal intensity as a function of time from an ROI placed within the proximal intracranial branch of the MCA. The start-stop interval is used to define the mean baseline signal intensity, while the stop-last interval represents the first pass of the contrast bolus. Note that subsequent decreases in signal intensity occur as the contrast material is recirculated.

B, Gamma-variate fit (*solid line*) to the baseline subtracted and inverted data (*dashed line*). The two variables used to quantify the curve are the first moment of the gamma-variate fit, termed the first-moment transit time (TT_{FM}), and the area under the fitted curve (relative cerebral blood volume [rCBV]).

rCBV were also expressed as the interhemispheric cerebral blood volume ratio, $rCBV_R$, for a particular hemodynamic ROI between the symptomatic (stented) and asymptomatic hemispheres for any one hemodynamic anatomic ROI (ACAT, MCAT1, MCAT2, or PCAT), as shown in Equation 5:

$$5) \qquad rCBV_R = rCBV_{symptomatic}/rCBV_{asymptomatic}.$$

Values were also expressed for the TT_{FM} as the interhemispheric difference (in seconds), as determined with Equation 6:

$$6) \qquad \Delta TT_{FM} = TT_{FMsymptomatic} - TT_{FMasymptomatic}.$$

Statistical Analysis

Comparisons of rCBV and TT_{FM} values between hemispheres obtained during any one imaging episode and of $rCBV_R$ and ΔTT_{FM} values before and after stenting were performed by using paired *t* tests after normality had been tested for. Direct comparisons of intersubject TT_{FM} and rCBV were not undertaken, as this technique is not quantitative. That is, *k* in Equation 1 was treated as an unknown and arbitrarily set to unity.

PTA and Stent Insertion

In all cases, the stenotic ICA corresponding to the patient's symptomatic side was treated. During the interventional procedure, a diagnostic angiographic catheter was placed in the common carotid artery from a standard femoral arterial approach, and then a wire (Compas; Mallinckrodt Medical Ltd, Northampton, UK) was used to access the external carotid artery. This step was followed by the placement of an 80–100-cm-long 7F sheath (Arrow International, Reading, PA) into the common carotid artery, followed by the administration of 1.2 mg of atropine. A 0.018-inch guidewire (V18; Boston Scientific, Natick, MA) was used to negotiate the stenosis into the ICA. Prestenting dilation was achieved by inflating a 3- or 4-mm-diameter balloon once for approximately 15 seconds. A 7- or 9-mm-diameter carotid Wallstent (Boston Scientific) was then deployed. Postdilation was achieved by using a balloon of 4 or 5 mm diameter inflated once for approximately 15 seconds.

Results

Good-quality or excellent perfusion data were acquired in all cases for both imaging episodes by using the subjective assessments of the time-intensity curves previously proposed (13). Sample data are shown in Figure 3. Perfusion data are summarized in Table 2.

Before Intervention

No statistically significant differences were observed between group mean interhemispheric rCBV values in any of the four vascular territories. Mean TT_{FM} was symmetrical in the PCAT and ACAT between the ipsilateral and contralateral hemispheres (mean ΔTT_{FM}, −0.14 and 0.12 seconds, respectively). Mean TT_{FM} was significantly longer in the ipsilateral, symptomatic hemisphere than in the contralateral, asymptomatic hemisphere in the MCAT1 (mean ΔTT_{FM}, 1.31 seconds and $P < .005$) and MCAT2 (mean ΔTT_{FM}, 1.09 seconds; $P < .005$).

After Intervention

As was the case before intervention, no statistically significant interhemispheric differences in rCBV were detected. Likewise, no significant asymmetry was detected in the TT_{FM} within the PCAT and ACAT (mean differences, −0.02 and 0.16 seconds, respectively). Smaller (than preintervention values), but still statistically significant interhemispheric asymmetry in mean TT_{FM} was found in the MCAT1 (mean difference, 0.51 seconds; $P < .05$) and MCAT2 (mean difference, 0.57 seconds; $P < .05$).

The observed decrease in TT_{FM} asymmetry after angioplasty and stent placement (61% in MCAT1 and 48% in MCAT2) was statistically significant within the MCAT1 (mean ΔTT_{FM} decreased by 0.8 seconds; $P < .05$).

Complex changes in rCBV were also present but not statistically significant. These included changes in the postinterventional mean $rCBV_R$ of up to 10% in the MCAT1 and ACAT. However, these were associated with large intragroup standard deviations (more than 50% in the ACAT).

Leptomeningeal Enhancement

Enhancement within the leptomeninges in symptomatic MCA territory was observed in eight of 11 cases. A small difference between mean $rCBV_R$ (the ratio between enhancing and contralateral nonenhancing areas) determined before and after stenting was not statistically significant (mean, 1.07 ± 0.25

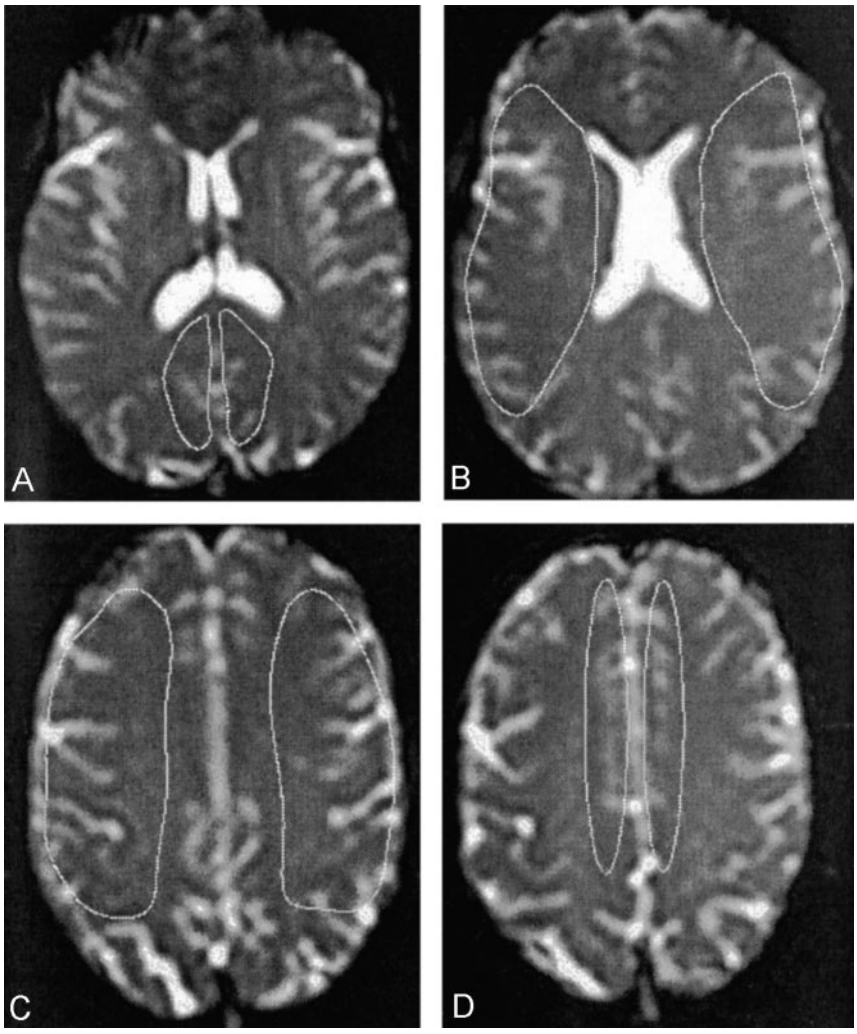

FIG 2. Placement of the ROIs.
A, PCAT.
B, MCAT1.
C, MCAT2.
D, ACAT.

before and 1.01 ± 0.18 after). Statistically significant interhemispheric asymmetry in mean TT_{FM} was found in areas of enhancement when compared with contralateral nonenhancing regions before intervention (mean difference, 1.31 seconds; $P < .05$). After stent placement, this difference declined and was no longer statistically significant (0.64 seconds; $P > .05$).

Discussion

The relative degree to which changes in intracerebral perfusion and the distal migration of particulate emboli effect stroke risk is uncertain. It is generally agreed, however, that intracerebral hemodynamics play an important role in disease progression and outcome. Several reports have documented abnormalities in cerebral perfusion in patients with ICA stenosis and occlusion, as measured by means of dynamic exogenous contrast MR susceptibility mapping (14–18). There are limited published data concerning the assessment of capillary bed perfusion in the context of carotid intervention (19–22). To our knowledge, this is the first report of the use of such a technique to monitor the acute (<3 hours) hemodynamic consequences of intervention in carotid disease.

To quantify flow in the capillary bed, two parameters are often used: localized blood volume and flow. These are related to each other by the mean transit time, according to the central volume principle: flow = volume/transit time. (For a review of these concepts, see the article by Griffiths et al [23]). When purely intravascular tracers are imaged, the mean transit time cannot be calculated in a straightforward manner from the first moment of a concentration time curve, as the first moment is related to the second moment which has a dependence on vascular topology (24). To highlight this concept, we denoted the first moment of the calculated concentration time curve as TT_{FM} rather than the mean transit time. TT_{FM} has a high dependence on mean transit time, and therefore, it does provide information about the temporal characteristics of tissue perfusion.

No attempt was made to quantitate CBV (based on knowledge of the arterial input), and thus, relative values were obtained and compared. There were no significant differences in rCBV between symptomatic and asymptomatic vascular territories or in $rCBV_R$ values before and after treatment. However, large interhemispheric differences and changes over time were apparent, but no patterns were detected with

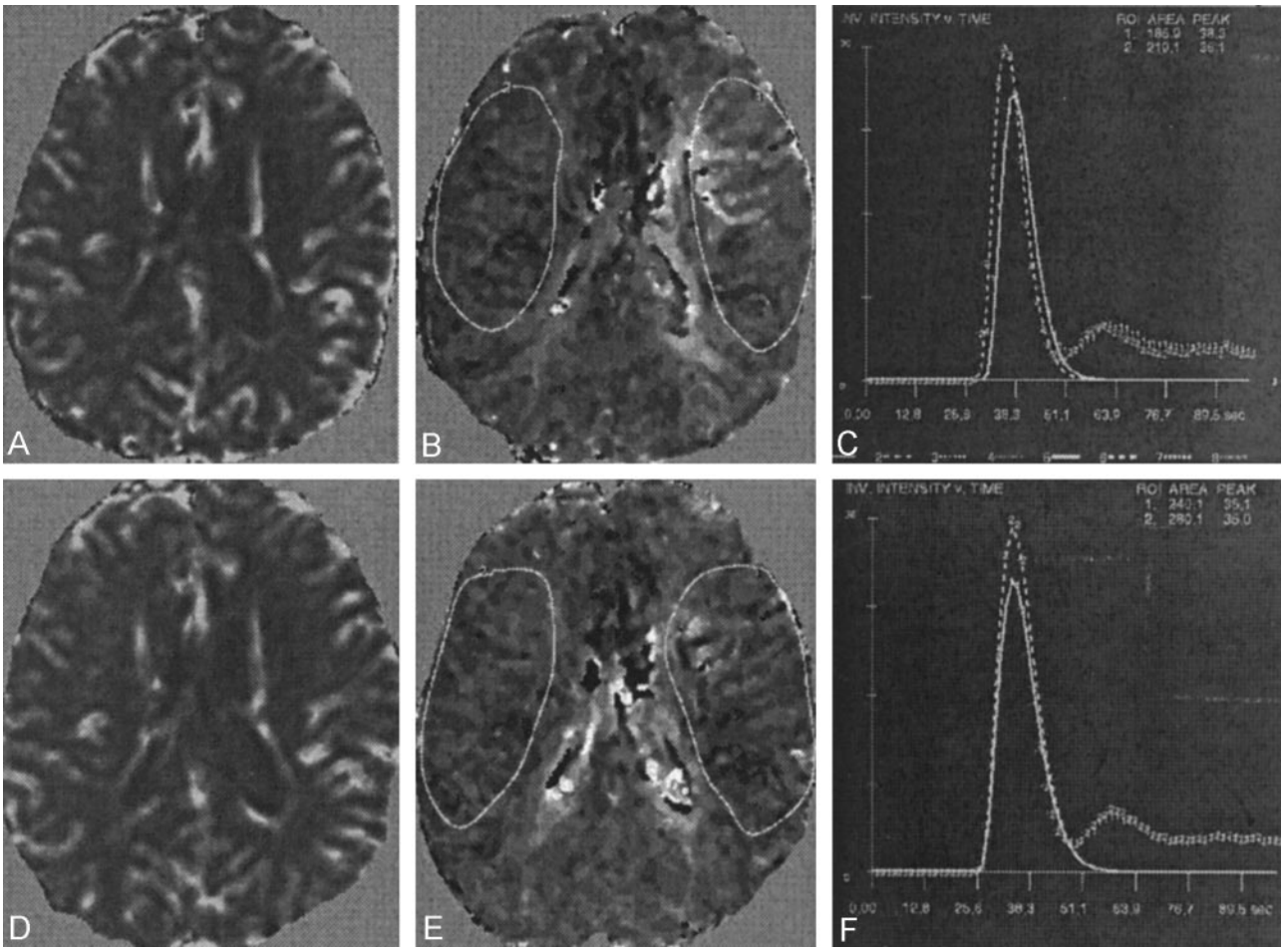

FIG 3. Perfusion data obtained at the level of the lateral ventricles in a patient with a symptomatic 95% stenosis in the left ICA and a 50% stenosis of the contralateral ICA.

A, Preintervention rCBV map.

B, Preintervention TT_{FM} map.

C, Gamma-variate fits corresponding to the depicted regions show a longer TT_{FM} and a smaller rCBV in the symptomatic hemisphere.

D, Postintervention rCBV map.

E, Postintervention TT_{FM} map.

F, Corresponding gamma-variate fits. Note the resolution of interhemispheric asymmetry in TT_{FM}.

TABLE 2: Perfusion Data Before and After Treatment

	$rCBV_R$		ΔTT_{FM}, seconds	
ROI	Before Intervention	After Intervention	Before Intervention	After Intervention
PCAT	0.98 ± 0.17	0.96 ± 0.26	−0.14 ± 0.42	−0.02 ± 0.68
MCAT1	1.01 ± 0.19	0.91 ± 0.18	1.31 ± 1.15*	0.51 ± 0.61†‡
MCAT2	1.06 ± 0.27	1.00 ± 0.13	1.09 ± 0.90*	0.57 ± 0.75†
ACAT	1.11 ± 0.36	1.01 ± 0.51	0.12 ± 0.64	0.16 ± 0.66

Note.—Data are the mean ± standard deviation. For cases of inter-hemispheric symmetry, the $rCBV_R$ was 1, and ΔTT_{FM} was 0 seconds.

* Statistically significant interhemispheric asymmetry in mean TT_{FM}, $P < .005$.

† Statistically significant interhemispheric asymmetry in mean TT_{FM}, $P < .05$.

‡ Significant difference in mean ΔTT_{FM} before and after intervention, $P < .05$.

respect to the symptomatic side or imaging time points. Some previous reports have documented statistically significant differences in interhemispheric blood volumes in carotid stenosis or occlusion (17, 21, 22), whereas others have not (15, 18, 20). Relative interhemispheric blood volume is a complex entity that may be influenced by the presence of other parameters, such as the status of the asymptomatic ICA and the vascular connectivity in the circle of Willis. One prominent feature observed in the present study is the degree of variation and change in rCBV and $rCBV_R$ within the ACAT. This observation may reflect the role that this supply has in collateral redistribution in vascular disease.

Bolus transit time, as indicated by TT_{FM}, did not vary significantly between hemispheres within the

ACAT or PCAT. This finding is expected in many cases because the areas may not be directly supplied by the ipsilateral ICA. The significant interhemispheric differences observed between MCA territories before intervention are in agreement with most (15, 18, 20) but not all (25) published results. These discrepancies may reflect different cohort characteristics, most notably degrees of stenoses in both symptomatic and asymptomatic supply arteries. The standard deviations in the mean TT_{FM} within this study may result from this variation and imply the existence of a complex multiparameter-dependant threshold at which changes in flow become physiologically important.

Data obtained before and after carotid stent placement demonstrated a significant reduction in mean TT_{FM} interhemispheric asymmetry (48% and 61% at the two MCA levels studied) within 3 hours of stent placement. Other published studies report normalization of perfusion parameters after 3 months (n = 13) (21) and 2–6 months (n = 19) (22). Cerebral CO_2 reactivity has been shown to increase by approximately 30% after 2 days and by 50% at 2 months after PTA, to a degree similar to that observed with endarterectomy (26). Further studies are needed to elucidate whether ΔTT_{FM} continues to change during a similar time scale.

Previously reported "unilateral leptomeningeal enhancement" observed after carotid stent insertion (10) was identified in eight of the 11 patients in the present study. The cause of this enhancement is, as yet, unidentified. Since the enhancement occurred within areas supplied by the symptomatic MCA, the observed changes in ΔTT_{FM}, which followed those in the MCAT1 and MCAT2 ROIs, were expected. Although no significant changes in localized blood volume were identified within areas of leptomeningeal enhancement (relative to contralateral parenchyma), the changes in TT_{FM} are likely to be indicative of increases in arterial inflow to symptomatic MCA territory, and this may be a contributory factor to the development of localized enhancement. A lack of vasodilatory response or capability may result in the inability to detect significant changes in rCBV.

Although not encountered in the group of patients studied here, $rCBV_R$ and TT_{FM} may also provide information regarding the nature of or perhaps a prognostic marker for the hyperemia syndrome (27) when measured at such a short interval after stent placement. Our understanding of interhemispheric asymmetry in bolus transit time is far from complete and our inability to account for changes in rCBV on a per-patient basis highlight a need for further study in this area. One of the inclusion criteria for participation in this study was the demonstration of an absence of significant obstruction both upstream and downstream of the symptomatic ICA stenosis. If present, such tandem disease would alter the arterial input function to the supplied parenchyma and thus be a cofactor in TT_{FM} and its observed partial resolution after intervention. It would also seem plausible that, given the systemic nature of atherosclerotic disease, disease-induced changes in blood flow may be present, even in cases in which no significant tandem disease is identifiable at angiography. If so, this change is also likely to influence measurement of TT_{FM} asymmetry, albeit to a lesser degree. Increased knowledge of other possible factors of influence may further our understanding of the effects of carotid stenosis on brain perfusion and its relationship to stroke risk. Such factors include normal variations in macrovascular topography and its relationship to spin history, the provision of contralateral blood supply (variants in the anatomy of the circle of Willis), arterial input to the brain (including cardiac output in patients who have atherosclerotic disease and whether brain vascular regulation is closely coupled with cardiovascular output), and the vasodilatory response in patients with carotid vascular disease.

Absolute quantitation of parenchymal perfusion (blood transit time, rCBV, and hence blood flow) has numerous potential advantages over the relative measures reported here. However, because of the numerous unknown cofactors outlined above, absolute quantitation is rather difficult. The potential advantages of a fully quantitative approach include 1) a reduction in the measurement error introduced by the expression of results in terms of ratios or differences; 2) the ability to make direct interindividual cross-sectional and intraindividual longitudinal comparisons; and, 3) with a combination of other MR techniques, the possible determination of localized oxygen extraction.

Conclusion

MR perfusion, as assessed by using an exogenous contrast agent, appears to be a marker for the acute cerebral hemodynamic sequelae of intervention in carotid disease. With this technique, short-term partial resolution of the timing asymmetry in interhemispheric perfusion after angioplasty and stent insertion for severe ICA stenosis has been demonstrated. Areas of leptomeningeal enhancement appear not to be associated with localized blood volume changes over the time scale of this investigation. Parenchymal MR perfusion assessment may provide an important indicator of the relative hemodynamic efficacy of different interventional techniques. Further long-term follow-up data are needed to determine the cerebral hemodynamic outcome of carotid stent placement.

Acknowledgments

The authors wish to thank the radiographers of the University of Sheffield MR imaging unit and the radiographers and nurses of the angiographic suite of the Royal Hallamshire Hospital for their expert assistance. Fruitful technical discussions between I.D.W. and Mr Wayne Dannels of Philips Medical Systems were appreciated.

References

1. North American Symptomatic Carotid Endarterectomy Trial Collaborators. **Beneficial effects of carotid endarterectomy in symptomatic patients with high grade carotid stenosis.** *N Eng J Med* 1991;325:445–453

2. European Carotid Surgery Trials Collaborative Group. **Randomised trial of endarterectomy for recently symptomatic carotid stenosis: final results of the MRC European Carotid Surgery Trial (ECST).** *Lancet* 1998;351:1379–1387
3. CAVATAS investigators. **Endovascular versus surgical treatment in patients with carotid stenosis in the carotid and vertebral artery transluminal angioplasty study (CAVATAS): a randomized study.** *Lancet* 2001;357:1729–1737
4. Yadav JS, Roubin GS, Iyer S, et al. **Elective stenting of the extracranial carotid arteries.** *Circulation* 1997;95:376–381
5. Caplan LR, Hennerici M. **Impaired clearance of emboli (washout) is an important link between hypoperfusion, embolism and ischaemic stroke.** *Arch Neurol* 1998;55:1475–1482
6. Weinmann HJ, Brasch RC, Press WR, Westbey GE. **Characteristics of gadolinium-DTPA complex: a potential NMR contrast agent.** *AJR Am J Roentgenol* 1984;142:619–624
7. Edelman RR, Mattle HP, Atkinson DJ, et al. **Cerebral blood flow: Assessment with dynamic contrast-enhanced T2*-weighted MR imaging at 1.5T.** *Radiology* 1990;176:211–220
8. Ostergaard L, Weisskoff RM, Chesler DA, Gyldensted C, Rosen BR. **High resolution measurement of cerebral blood flow using intravascular tracer bolus passages, I: mathematical approach and statistical analysis.** *Magn Reson Med* 1996;36:715–725
9. Ostergaard L, Sorenson AG, Kwong KK, Weisskoff RM, Gyldensted C. **High resolution measurement of cerebral blood flow using intravascular tracer bolus passages, II: experimental comparison and preliminary results.** *Magn Reson Med* 1996;36:726–736
10. Wilkinson ID, Griffiths PD, Hoggard N, Cleveland TJ, Gaines PA, Venables GS. **Unilateral leptomeningeal enhancement after carotid stent insertion detected by MR imaging.** *Stroke* 2000;31:848–851
11. Benner T, Heiland S, Erb G, Forsting M, Sartor K. **Accuracy of gamma-variate fits to concentration-time curves from dynamic susceptibility-contrast enhanced MRI: influence of time resolution, maximal signal drop and signal-to-noise.** *Magn Reson Imaging* 1997;15:307–317
12. Starmer CF Clark DO. **Computer computations of cardiac output using the gamma function.** *J Appl Physiol* 1970;28:219–220
13. Griffiths PD, Wilkinson ID, Wels T, Hoggard N. **Brain MR perfusion imaging in humans: advantages of high-molarity gadolinium chelates.** *Acta Radiologica* 2001;42:555–559
14. Kim JH, Lee SJ, Shin T, et al. **Correlative assessment of hemodynamic parameters obtained with T2*-weighted perfusion MR imaging and SPECT in symptomatic carotid artery occlusion.** *AJNR Am J Neuroradiol* 2000;21:1450–1456
15. Nighoghossian N, Berthezene Y, Phillippon B, Adeleine P, Froment JC, Trouillas P. **Hemodynamic parameter assessment with dynamic susceptibility contrast magnetic resonance imaging in unilateral symptomatic internal carotid artery occlusion.** *Stroke* 1996;27:474–479
16. Nasel C, Azizi A, Wilfort A, Mallek R, Schindler E. **Measurement of time-to-peak parameter by use of a new standardization method in patients with stenotic or occlusive disease of the carotid artery.** *AJNR Am J Neuroradiol* 2001;22:1056–1061
17. Lythgoe DJ, Ostergaard L, William SC, et al. **Quantitative perfusion imaging in carotid artery stenosis using dynamic susceptibility contrast-enhanced magnetic resonance imaging.** *Magn Reson Imaging* 2000;18:1–11
18. Maeda M, Yuh WT, Ueda T, et al. **Severe occlusive carotid artery disease: hemodynamic assessment by MR perfusion imaging in symptomatic patients.** *AJNR Am J Neuroradiol* 1999;20:43–51
19. Gillard JH, Hardingham CR, Kirkpatrick PJ, Antoun NM, Freer CEL, Griffiths PD. **Evaluation of carotid endarterectomy with sequential MR perfusion imaging: a preliminary report.** *AJNR Am J Neuroradiol* 1998;19:1747–1752
20. Gillard JH, Hardingham CR, Antoun NM, Freer CE, Kirkpatrick PJ. **Evaluation of carotid endarterectomy with sequential MR perfusion imaging: a preliminary 12-month follow up.** *Clin Radiol* 1999;54:798–803
21. Doerfler A, Eckstein HH, Eichbaum M, et al. **Perfusion-weighted magnetic resonance imaging in patients with carotid artery disease before and after carotid endarterectomy.** *J Vasc Surg* 2001;34:587–593
22. Kluytmans M, van der Grond J, Eikelboom BC, Viergever MA. **Long-term hemodynamic effects of carotid endarterectomy.** *Stroke* 1998;29:1567–1572
23. Griffiths PD, Hoggard N, Dannels W, Wilkinson ID. **In vivo measurement of cerebral blood flow: a review of methods and applications.** *Vasc Med* 2001;6:51–60
24. Weisskoff RM, Chesler D, Boxerman JL, Rosen BR. **Pitfalls in Mr measurement of tissue blood flow with intravascular tracers: which mean transit time?** *Magn Reson Med* 1993;29:553–559
25. Bozzao A, Floris R, Gaudiello F, Finocchi V, Fantozzi LM Simonetti G. **Hemodynamic modifications in patients with symptomatic unilateral stenosis of the internal carotid artery: evaluation with MR imaging perfusion sequences.** *AJNR Am J Neuroradiol* 2002;23:1342–1345
26. Markus HS, Clifton A, Buckenham T, Taylor R, Brown MM. **Improvement in cerebral hemodynamics after carotid angioplasty.** *Stroke* 1996;27:612–616
27. Powers AD, Smith RR. **Hyperperfusion syndrome after carotid endarterectomy: a transcranial Doppler evaluation.** *Neurosurgery* 1990;26:56–59